JOURNAL OF MATERIALS SCIENCE 29 (1994) 1795–1800

Fabrication of thin oxide coatings on ceramic fibres by a sol–gel technique

D. B. GUNDEL, P. J. TAYLOR, F. E. WAWNER
Department of Materials Science and Engineering, University of Virginia, Charlottesville, VA 22903, USA

Various metal oxides are potential reaction barriers in titanium/silicon carbide composites. A sol–gel process utilizing metal alkoxides was developed to coat silicon carbide fibres with relatively thick, crack-free, adherent layers of yttrium and calcium oxide. A multiple-dip technique was employed in order to avoid cracking due to large residual thermal and drying stresses produced in the film. The influence of several processing parameters and the geometry of the substrate on the coating thickness is discussed.

1. Introduction

When titanium–matrix composites are exposed to sufficiently high temperatures, the fibre and the matrix react to form brittle reaction products at the fibre–matrix interface. The presence of these compounds can lower the longitudinal tensile strength of the fibre, and hence the composite [1, 2]. There is, therefore, great interest in inhibiting the reaction by placing compounds between the fibre and matrix to act as reaction barriers. Candidate materials for this purpose include metal oxides such as yttria (yttrium oxide) and calcia (calcium oxide) [3–5].

Several means are currently available to deposit ceramic materials on fibres, including chemical vapour deposition (CVD), sputtering, and sol–gel techniques [6]. CVD is a common method for the production of thin films of ceramic materials on fibres, but requires specialized equipment and is fairly expensive. Sputter deposition has reportedly been employed to deposit Y_2O_3 on to SiC fibres [5, 7, 8], but again the necessary facilities for the process are not always readily available. A related procedure to produce an oxide layer is to first coat the fibre with a metal (by sputter deposition, for example) then later heat it in an oxidizing atmosphere [5, 9]. Finally, sol–gel techniques have been successfully used to coat graphite fibres with both TiO_2 and silicate-based ceramics [10, 11]. In terms of simplicity and expense, sol–gel is probably the most favourable of these methods to evaluate candidate reaction barrier coatings.

The sol–gel process is becoming increasingly important for the production of thin films due to the wide variety of technologically important coatings that can be prepared [12–14]. A thorough review of sol–gel techniques in general, including the creation of thin films, is given by Brinker and Scherer [12]. Sol–gel processing using organometallic precursors involves the hydrolysis of a metal alkoxide to form a gel which is later pyrolysed at high temperatures to yield the desired compound.

One of the primary problems associated with films produced using this technique is that they often contain cracks owing to large internal stresses produced during fabrication. Cracks in the coating are unacceptable for the intended use because they provide fast diffusion paths for reacting species and may allow the fibre and matrix to come into direct contact. Stresses include those due to drying and sintering of the film, and those resulting from unequal coefficients of thermal expansion (CTE) of the fibre and coating. If the sum of these stresses is greater than the strength of the coating, cracking is expected.

The multiple-dip technique is a practical method to obtain mechanically stable coatings because thin layers have lower drying/sintering stresses [15] and contain a characteristically smaller flaw-size distribution than do thicker layers. The empirical observation is that films thicker than 200–1000 nm crack, whereas thinner ones can be produced without cracks [10, 12, 15]. Another advantage of this technique is that surface defects on the coating may be covered by successive layers, thereby "healing" the flaw. Although dipping a component several times will increase the overall cost of coating in a large-scale process, this may be the only way to completely to avoid cracking. Alternatives include drying the liquid film and allowing it to gel, then recoating several times, until finally calcining the resultant thick gel layer. This is attractive in that the intermediate pyrolysation steps are deleted, but large drying and sintering stresses may still be generated.

The purpose of this investigation was to determine the feasibility of placing thin metal oxide films on reinforcing fibres using metal alkoxide precursors. The objective was to produce coatings approximately 1 μm thick that were uniform, adherent, and crack-free.

2. Experimental procedure

2.1. Materials

The SCS-6 fibre, manufactured by Textron Specialty Materials (Lowell, MA), was used as a substrate for the coatings. This fibre was approximately 140 μm

0022–2461

TABLE I Compound properties

	Density ($g ml^{-1}$)	Mol. wt ($g mol^{-1}$)	Reference
Yttrium methoxyethoxide	1.01 (15%–18% in MOE)	314.17	Gelest Inc.
Calcium methoxyethoxide	1.01 (20% in MOE)	190.25	Gelest Inc.
Yttrium oxide (Y_2O_3)	5.01	225.81	[18]
Calcium oxide (CaO)	3.32	56.08	[18]

diameter and already had a 3–5 μm thick carbon-rich ("SCS") coating on its surface. The structure of this type of fibre has been studied by Nutt and Wawner [16] and more recently by Ning and Pirouz [17]. Prior to dipping, the fibre was prepared by thorough cleaning with an organic solvent, followed by heating to 800 °C in air for a short period. The starting metal alkoxides used were yttrium and calcium methoxyethoxide obtained in concentrations of 15%–18% and 20% (wt %) in methoxyethanol (MOE), respectively, from Gelest Inc. (Tullytown, PA). Using the data from Table I the concentration of the original solutions was calculated to be 0.48–0.58 $mol l^{-1}$ (M) and 1.1 M for the yttrium and calcium alkoxides, respectively. These solutions were further diluted with ethanol in order to yield oxide coatings of the desired thickness. This solvent was chosen because of its ability to completely wet the fibre surface and therefore produce more uniform coatings.

2.2. Coating process

The approach taken in this study to obtain crack-free coatings was to put a large number of very thin oxide layers on the fibre successively. Each individual layer was produced by dipping the fibre bundle into the alkoxide solution, evaporating the solvent, allowing the alkoxide to hydrolyse by reaction with water in the laboratory air (gelation), and finally calcining the gel at high temperatures in air (600 and 700 °C for the yttria and calcia, respectively). The fibres were coated in a small batch process using a vertical translation system that withdrew them from the solution at a rate of 7.7 $cm s^{-1}$. The target oxide thickness per dip was 10–50 nm. According to other researchers, this is well below the range where no cracks are observed in sol–gel prepared films [10, 12, 15].

2.3. Coating characterization

Observations of the coated fibres were performed with a Jeol JSM-35 scanning electron microscope (SEM). Measurements of the coating thicknesses were made using scanning electron micrographs of the fibre cross-sections.

In order to determine if the desired coatings were produced, 1 cm^2 pieces of amorphous quartz plate were coated in nearly the same manner as the fibres. Thicker coatings, expected to yield stronger diffraction peaks, were deposited on the quartz substrates by using slightly more concentrated alkoxide solutions than used to coat the fibres. In addition, because the quartz pieces were much larger than the fibres, longer hold times at the high temperatures were necessary to ensure that the gel completely converted to the oxide. They were then placed in a Scintag Inc. XDS-2000 Theta/Theta X-ray Diffractometer and the resulting diffraction patterns were compared to those contained in the International Center for Diffraction Data (ICDD, Swarthmore, PA) powder diffraction database to identify the compounds present.

3. Results

3.1. Coating characterization

The results of the X-ray diffraction experiments are given in Fig. 1. These coatings yielded patterns that were consistent with the ICDD standard powder patterns of yttria (Y_2O_3) and calcia (CaO). Although this indicates that the quartz pieces were coated with the desired compounds, the oxide films were often severely cracked and tended to flake off the substrate.

In general, the coatings obtained on the fibres were uniform, adherent, and crack-free. In a few isolated cases, the coating was uneven and cracked when the fibres were allowed to touch during the evaporation and pyrolysation steps. Fig. 2 shows typical scanning electron micrographs of the yttria coating obtained in this study. Fig. 2a and b are micrographs taken using backscattered electrons to enhance the contrast between the fibre and coating. The cross-section in Fig. 2a was prepared simply by pressing on the fibre with a sharp edge until it fractured. The coating only came off the fibre in a very small area, and closer examination revealed that the outer SCS coating was also missing. This, and the fact that the features of the fracture surface were continous across the SCS–yttrium oxide coating interface, indicate that the coating was very adherent. Fig. 2b shows a closer view of the coating and also gives an idea of its thickness as compared to the SCS coating. The surface of a yttria-coated fibre is shown in Fig. 2c. No cracks or pores could be observed over nearly the entire surface of the fibres studied (yttria or calcia), even at high magnifications (up to ×10 000). Based on observations of fibre cross-sections, the calcia coating was not as well bonded to the fibre as the yttria coating. Fig. 3 is a scanning electron micrograph of the calcia-coated fibre in which the oxide coating is clearly visible because the fracture surface is not continuous across the interface. The calcia coating often spalled off the fibre near to where it was fractured, and in general, the thicker the coating the less adherent it was.

3.2. Coating thickness

The effect of the alkoxide concentration and number of dips on the thickness of the resulting oxide layer was investigated in order to observe the general influence of these variables. Three different concentrations were studied for yttria and one was studied for calcia.

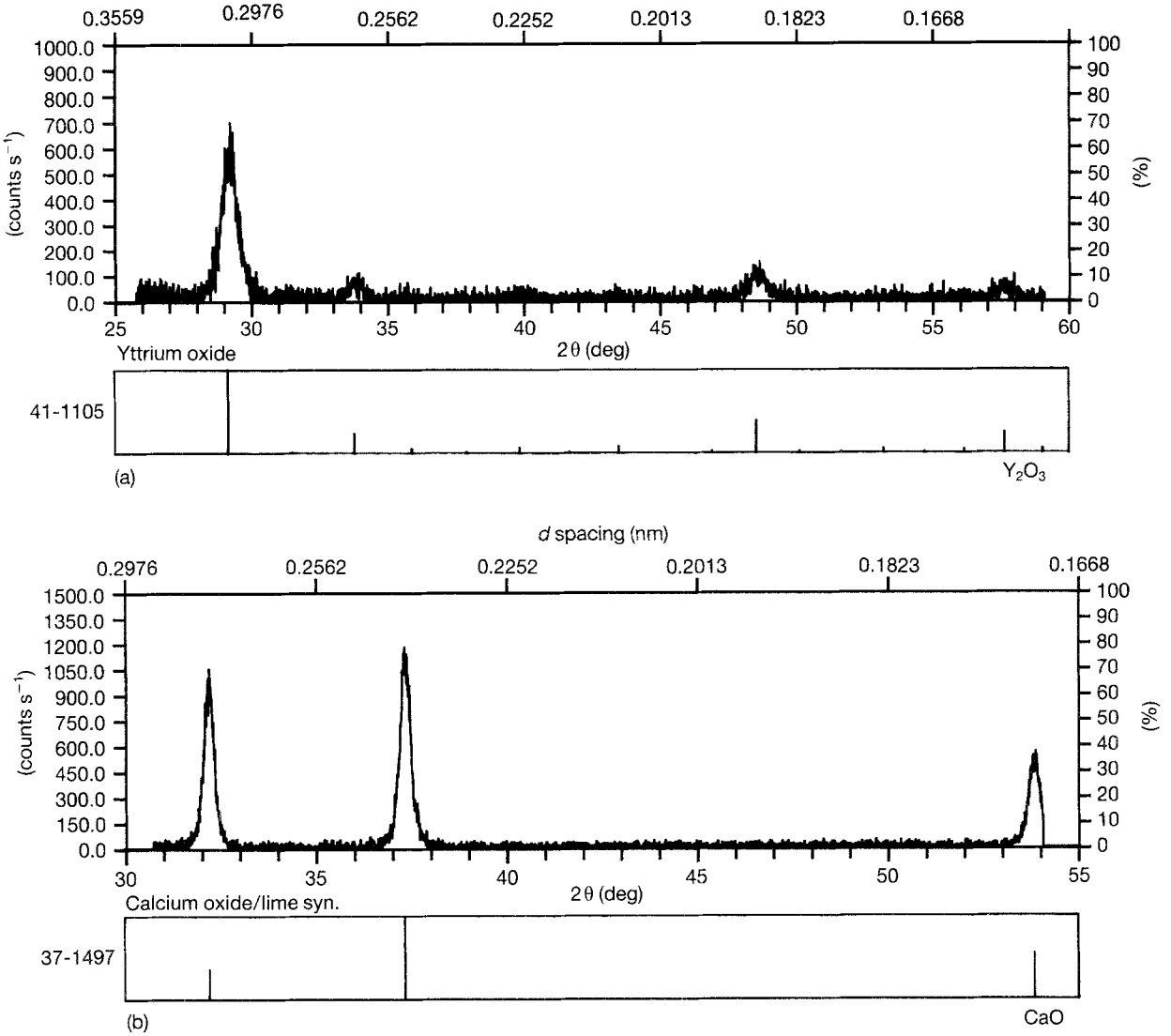

Figure 1 X-ray diffraction patterns of amorphous quartz coated with (a) yttrium oxide, and (b) calcium oxide. The intensity is plotted versus 2θ (bottom) and the *d*-spacing (top). The reference power patterns from ICDD (International Center for Diffraction Data) are also given.

Fig. 4 is a plot of the oxide thickness versus number of dips for three concentrations of the yttrium alkoxide. The trend observed was consistent with a linear dependence of coating thickness on alkoxide concentration and dip number that has been observed in other systems [10]. Table II lists the alkoxide concentration (assuming the initial yttrium alkoxide concentration to be 16.5 wt %) and slope of the linear least squares lines through the data.

4. Discussion

4.1. Residual thermal stresses

Due to the coefficient of thermal expansion (CTE) mismatch between the fibres and the coatings in the present case, significant thermal residual stresses will be generated in the coating upon cooling from the calcification temperature. Expressions derived for thermal stresses generally indicate that their magnitude is directly proportional to the difference in CTEs, $\Delta\alpha$ and the temperature change, ΔT. A simplified expression for the stress in a thin film, σ_f, on a substrate has been reported by Knorr [19]

$$\sigma_f = \frac{E_f}{(1 - \nu_f)} \Delta\alpha\Delta T \quad (1)$$

The terms ν_f and E_f are, the Poisson's ratio and Young's modulus of the film, respectively. The residual stresses are, therefore, mainly dependent on the modulus of the coating material, the CTEs of the components and the temperature change. The average CTEs for silicon carbide, calcia and yttria in the temperature range of interest are roughly 4.5, 13, and 8.2 $\mu m\, m^{-1}\, °C^{-1}$ [20], respectively. In the particular case of a coated cylinder, given these CTEs, the axial as well as the circumferential stresses will be tensile in nature while the radial stress will be compressive upon cooling. Equation 2 was derived for a flat substrate but can be used to estimate the axial tensile stress. It is assumed that there are no thermal stresses at the high temperature in order to apply this equation to the case of sol–gel prepared films, but in reality there may be significant residual drying/sintering stresses after the oxide has formed. The drying/sintering stresses will also have this same sign (tensile or compressive) with respect to orientation. The modulus of yttria is 169 GPa [20] and that for calcia is not available, but is expected to be in the range of 100–400 GPa, and can be assumed to be about 250 GPa for the present discussion. Thus the thermal stresses are expected to be much larger in the calcia coating than the yttria

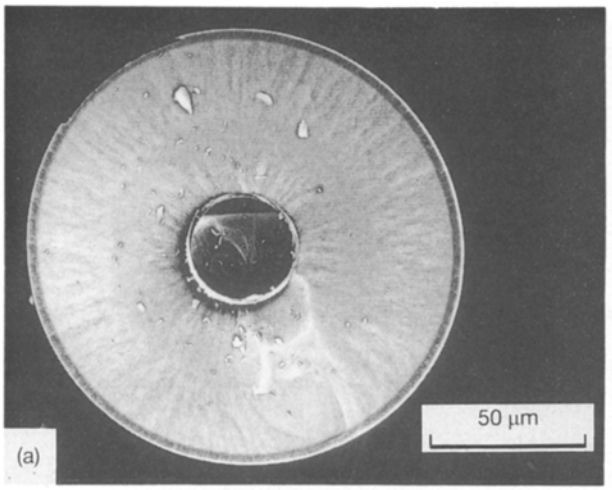

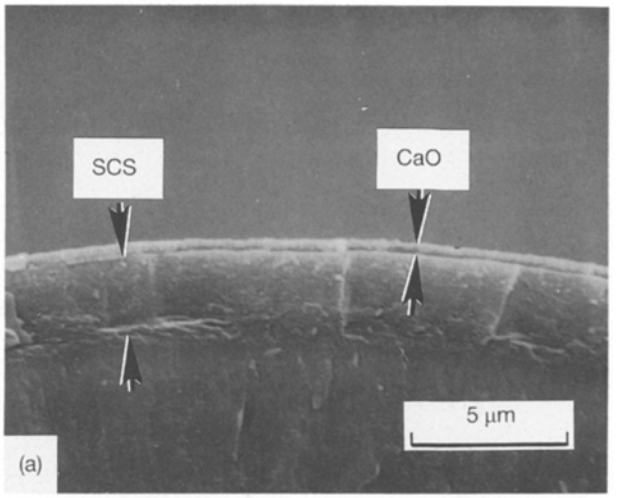

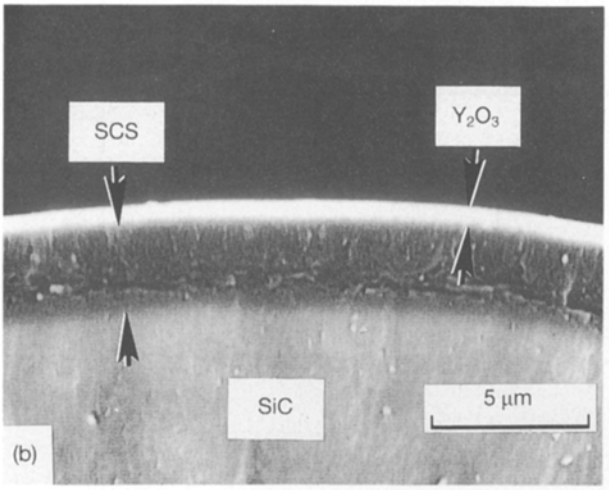

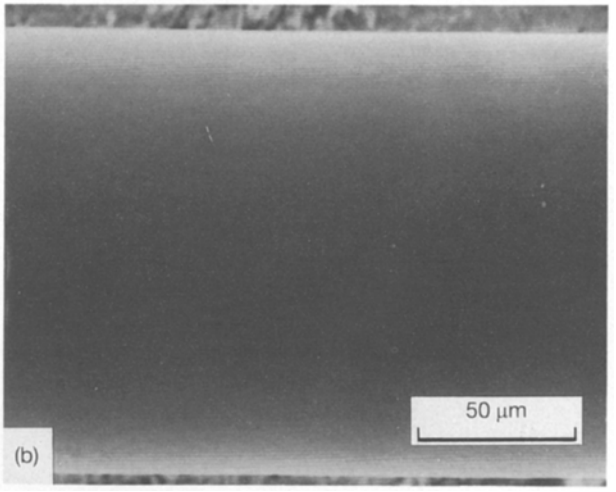

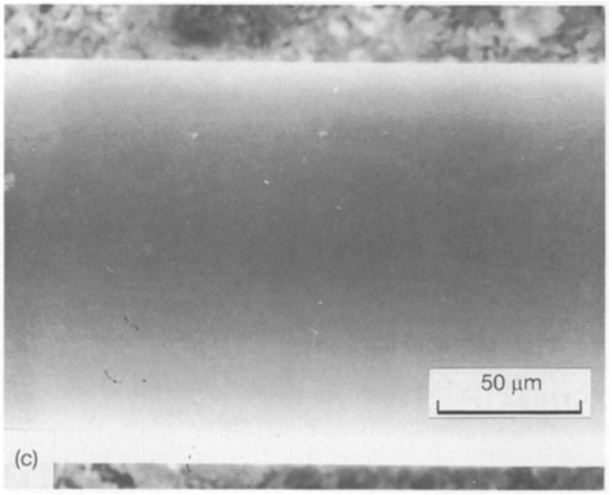

Figure 2 Scanning electron micrographs of the yttrium oxide coating on SCS-6 fibre: (a, b) backscattered electron images (BEI) of the fibre cross-section, and (c) a secondary electron image (SEI) of the fibre surface. BEI clearly highlights the yttria coating.

Figure 3 SEM backscattered electron image of the calcia coating on SCS-6. It tended to separate from the fibre more easily than the yttria coating. Note the fracture surface is not continuous across the SCS–calcia interface.

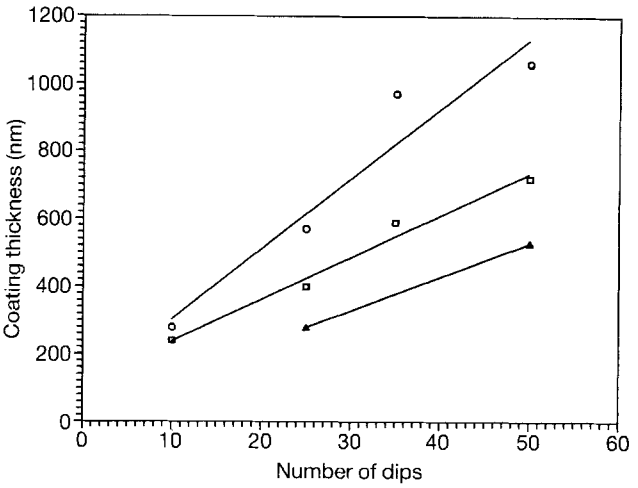

Figure 4 Coating thickness versus number of dips for three concentrations of yttrium methoxyethoxide solution: (○) 0.18 M, (□) 0.13 M, and (△) 0.066 M. The standard deviation of the measurements is approximately ± 10%.

coating, due to its greater CTE. This may suggest that the yttria coating will be more mechanically stable than calcia; however, other factors such as the coating flaw-size distributions and residual drying/sintering stresses also play a critical role in cracking behaviour.

As the coating increases in thickness, its internal stresses and effective strength are altered. The thermal stresses are not significantly mitigated by the relatively small increase in coating thickness produced during this investigations; however, the size of the largest flaws in the coating is proportional to the coating

TABLE II Solution data

Coating	Solution	Alkoxide concentration ($mol\,l^{-1}$)	Slope (nm/dip)	t, Equation 4 (nm/dip)
Yttira	1	0.18	21	5.1
	2	0.13	13	3.8
	3	0.066	10	1.9
Calcia	1	0.11	24	2.3

volume (or its thickness) and therefore the probability of the residual stresses exceeding the failure strength of the coating increases rapidly with coating thickness. The multiple dip technique does not lessen the thermal residual stresses in the coating as its thickness is increased, but ideally limits the drying/sintering stresses to the very outer layer thereby reducing the likelihood that a through-thickness crack will form.

4.2. Coating mechanical stability

The lack of mechanical stability of the coatings on the quartz was probably due to much higher stresses in these coatings than those on the fibres. The coating thickness per dip on the quartz was larger than on the fibres because of the higher alkoxide solution concentration and the flat nature of the surface (as opposed to the sharply curved fibre surface – discussed below). As described previously, the thicker layers per dip will give rise to much larger drying/sintering stresses. In addition, the thermal stresses in this system are expected to be greater than those on the coated fibre because of the lower CTE of quartz (CTE SiO_2 $= 1.14\,\mu m\,m^{-1}\,°C^{-1}$ [20]). It is possible that the combined effects of these two sources of internal stress are responsible for the observed cracking and delamination.

The separation of the calcium oxide from the fibre upon fracture may be indicative of a weak coating/fibre bond or high residual tensile stresses in the coating. Using the values above ($v_f = 0.3$) and Equation 1, the stress can be calculated to be on the order of 2000 MPa upon cooling from the calcification temperature (700 °C). When a fibre is fractured in order to expose the cross-section, the longitudinal film (thermal) stresses near the edge can be relaxed if the coating delaminates from the fibre. This separation is expected to give rise to the observed discontinuous fracture surface across this interface. A weaker bond here may facilitate the delamination, as will localized cracking of the film. Presumably the discontinuity across the oxide coating/fibre interface was not observed for the yttrium oxide coating because of lower film (residual thermal) stresses and possibly stronger bonding.

4.3. Coating thickness

The thickness of the resulting oxide layer on the fibre after a single dip is dependent upon the thickness of the layer of liquid that clings to the fibre immediately after dipping (the entrained liquid), which is in turn dependent upon several factors. For fibres the entrained layer of liquid is much thinner than that on a flat plate because of the sharp curvature of the substrate's (hence the liquid's) surface. This effectively adds a new force to the system in addition to those discussed in the review by Scriven [21], where the dipping of flat plates was described. The force due to the substrate curvature acts along with the gravitational force to thin the liquid layer and in opposition to the viscous force which tends to thicken it. This effect can lead to entrained liquid thicknesses that are several times smaller than on a flat plate.

The theoretical aspect of the dipping of wires has been studied by several researchers [22–25] with the best reported fit to experimental results for small diameter wires reported by White and Tallmadge [24]. Their results, however, according to the work of Goucher and Ward [26] and Gundel *et al.* [27], do not accurately model the thickness of the entrained layer with small diameter fibres and low fibre withdrawal speeds. The best available fit for fibre withdrawal in this regime is the empirical result reported by Goucher and Ward

$$h = 4.8\, r_o \left(\frac{\mu U}{\sigma}\right) \tag{2}$$

The entrained liquid layer thickness, h, is therefore dependent on the radius of the fibre (wire), r_o, the substrate withdrawal rate, U, the viscosity, μ, and surface tension, σ, of the solution. The term $\mu U/\sigma$ is known as the capillary number or the dimensionless withdrawal rate. Note that this equation does not include the gravitational term that becomes important only when thicker layers of fluid are entrained.

Equation 2 can be combined with expressions relating the alkoxide concentration to oxide thickness in order to arrive at a relationship for the thickness of oxide product per dip. Upon drying and calcification, the liquid on the fibre is converted to the oxide and undergoes a volume reduction which can be expressed by

$$V_{ox}C_{alk} = \frac{(r_o + t)^2 - r_o^2}{(r_o + h)^2 - r_o^2} \tag{3}$$

V_{ox} is the theoretical volume of oxide produced if 1 mol alkoxide is completely converted to product, C_{alk} is the concentration (molarity) of the alkoxide solution, and t is the thickness of the oxide layer per dip. If r_o is large compared to h (and t), then $V_{ox}C_{alk}$ will be approximately equal to t/h. Equation 2 can then be incorporated with this simplified expression to yield

$$t = 4.8\, V_{ox}C_{alk}\, r_o \left(\frac{\mu U}{\sigma}\right) \tag{4}$$

This equation predicts a linear relationship of t with the solution's molarity and viscosity, and the dip rate.

The variables in Equation 4 are known or can be approximated in order to calculate values of t. From data in Table I, V_{ox} was found to be 22.5 ml Y_2O_3/mol alkoxide and 16.9 ml CaO/mol alkoxide. The viscosity of ethanol, the main solvent used in the coating process, at room temperature is 1.1 mPa and its surface

tension is 22.3 mJ m^{-2} [18]. The predicted values of t are given in Table II, and they are several times smaller than those experimentally measured. The variable that is most probably responsible for the underprediction is the viscosity of the solutions. The alkoxide solutions were found to increase gradually in viscosity over time owing to partial gelation. The viscosities were not monitored in this study but could very well account for the higher observed thicknesses. To determine if Equation 4 is valid, a more thorough investigation must be undertaken using alkoxide solutions of known, unchanging properties.

4.4. Alkoxide solution stability

The alkoxide solutions did not always have a long shelf life, and sometimes irreversibly gelled within a matter of days. This was most probably the result of water vapour in the laboratory air entering the solution and hydrolysing the alkoxide. Methods to improve the lifetime of the solutions were not investigated in this study, but these would be necessary in any large-scale coating operation. Possible ways to solve this problem may include protecting the bulk solution from water vapour in the environment or adding chelating agents or acids to the alkoxide solution [14].

5. Conclusions

Simple oxide coatings of yttrium (Y_2O_3) and calcium (CaO) were obtained by a sol–gel route using alkoxide precursors. The coatings were deposited on small-diameter ceramic fibres using a multiple-dip technique that led to films that were, in general, relatively thick, uniform, adherent, and crack-free. The general influence of alkoxide concentration and number of dips on the coating thickness was studied. An equation relating the oxide thickness per dip to various parameters (assuming complete conversion of the metal in the alkoxide to the oxide) was applied to this system and found to underestimate the experimentally determined thicknesses. This was most probably due to partial gelation of the alkoxide solution while dipping, which increased its viscosity. The technique developed here to deposit these films can possibly be employed to create a wide variety of other oxide coatings.

Acknowledgements

The assistance of T. McGarry with experimental work is greatly appreciated. The authors acknowledge the support of NASA, Langley Research Center, Grant NAG-1-745, D. L. Dicus and W. D. Brewer, contract monitors. The SCS-6 fibre was generously provided by Textron Specialty Materials Division, Lowell, MA.

References

1. A. G. METCALFE, in "Composite Materials", Vol. 4, edited by K. G. Kreider (Academic Press, New York, 1974).
2. S. OCHIAI and Y. MURAKAMI, *J. Mater. Sci.* **14** (1979) 831.
3. G. H. REYNOLDS and J. H. NORMAN, in "Proceedings of the Titanium Aluminide Workshop Conference", Orlando, FL, February 1991, edited by P. R. Smith, S. J. Balsone and T. Nicholas, Wright-Patterson Air Force Base, OH, May 1990, p. 96. (Report WL-TR-91-4020.)
4. G. H. REYNOLDS, J. H. NORMAN and W. E. BELL, *ibid.*, p. 202.
5. R. R. KIESCHKE, R. E. SOMEKH and T. W. CLYNE, *Acta Metall. Mater.* **39** (1991) 427.
6. D. C. CRANMER, in "Proceedings of 12th Annual Conference on Composites and Advanced Ceramic Materials", January 1988 (American Ceramic Society, OH, 1988) p. 1121.
7. R. R. KIESCHKE and T. W. CLYNE, *Mater. Sci. Eng.* **A135** (1991) 145.
8. K. BILBA, J. P. MANAUD, Y. LE PETITCORPS and J. M. QUENISSET, *ibid.* **A135** (1991) 141.
9. T. E. STEELMAN, R. H. LORENZ, G. R. MARTIN and R. P. ROBELLETO, "Silicon Carbide/Titanium Material and Process Fundamentals", AFWAL-TR-82-4306 (Wright-Patterson Air Force Base, OH, 1982).
10. J. P. CLEMENT, H. J. RACK, K. T. WU and H. G. SPENCER, *Mater. Manuf. Proc.* **5**(1) (1990) 17.
11. H. KATZMAN, US Pat. 4376804 (1983).
12. C. J. BRINKER and G. W. SCHERER, "Sol–Gel Science: The Physics and Chemistry of Sol–Gel Processing" (Academic Press, New York, 1990).
13. D. R. UHLMANN and G. P. RAJENDRAN, in "Ultrastructure Processing of Advanced Ceramics", edited by J. D. Mackenzie and D. R. Ulrich (Wiley, New York, 1988) p. 252.
14. G. YI and M. SAYER, *Ceram. Bull.* **70** (1991) 1173.
15. A. ATKINSON and R. M. GUPPY, *J. Mater. Sci.* **26** (1991) 3869.
16. S. R. NUTT and F. E. WAWNER, *ibid.* **20** (1985) 1953.
17. X. J. NING and P. PIROUZ, *J. Mater. Res.* **6** (1991) 2234.
18. D. R. LIDE (ed.), "Handbook of Chemistry and Physics", 71st Edn (CRC Press, Boca Raton, FL, 1990).
19. D. B. KNORR, *J. Metals* **44**(7) (1992) 29.
20. N. J. SHAW, J. A. DICARLO, N. S. JACOBSON, S. R. LEVINE, J. A. NESBITT, H. B. PROBST, W. A. SANDERS and C. A. STEARNS, "Materials for Engine Applications Above 3000 °F – an Overview", NASA Technical Memorandum 100169 (NASA Lewis Research Center, Cleveland, OH, 1987).
21. L. E. SCRIVEN, in "Better Ceramics Through Chemistry III", edited by C. J. Brinker, D. E. Clark and D. R. Ulrich (Materials Research Society, Pittsburgh, PA, 1988) p. 717.
22. J. A. TALLMADGE, R. A. LABINE and B. H. WOOD, *Ind. Eng. Chem. Fundamentals Q.* **4** (1965) 400.
23. D. A. WHITE and J. A. TALLMADGE, *AIChE J.* **12** (1966) 333.
24. *Idem, ibid.* **13** (1967) 745.
25. S. D. R. WILSON, *ibid.* **34** (1988) 1732.
26. F. S. GOUCHER and H. WARD, *Phil. Mag. 6th Ser.* **44** (1922) 1002.
27. D. B. GUNDEL, T. MCGARRY and F. E. WAWNER, unpublished research, University of Virginia (1992).

Received 14 December 1992
and accepted 31 August 1993